Increasing spatial and temporal resolution in energy system optimization model – the case of Kenya

Nandi Moksnes (nandi@kth.se)
KTH Royal Institute of Technology
Mark Howells
STEER Centre, Department of Geography & Environment, Loughborough University, UK
William Usher
KTH Royal Institute of Technology

Research Article

Keywords: Energy access, spatial, geospatial, OSeMOSYS, energy systems modelling, energy systems optimization modelling, sustainable development goals, SDG

Posted Date: June 8th, 2022

DOI: https://doi.org/10.21203/rs.3.rs-1734728/v1

Abstract

At the time of writing 759 million people (2019) still lack access to electricity globally. Energy planning is important to describe plausible pathways to achieve national goals, where energy systems models are tools to explore scenarios and provide insight. Until recently, modelling energy access in countries with a low electrification rate was conducted at low spatial (e.g. national) and/or temporal resolution (e.g. annual time slices or 'overnight' electrification). In this paper, we develop methods in an open-source computational workflow with high spatial and medium temporal resolution in OSeMOSYS. We use Kenya as our case application where still 16 million people lack access to electricity (2019). The spatial resolution of approximately 40x40km cells leads to 591 demand cells split between electrified and un-electrified. Results show that a key limitation of PV + battery systems is that they struggle to provide peak demand. This manifests itself in very high marginal costs at peak times. That high marginal cost drives a transition of the system to mini-grid and grid connections as soon as demand levels are high.

1. Introduction

Energy has for a long time been identified as an enabler for development. With the launch of the 17 sustainable development goals (SDG) clear targets has been set for Agenda 2030. SDG7 In particular universal access to modern energy, has been identified to be an enabler for education (SDG4), end poverty (SDG1), healthcare (SDG3), water and sanitation (SDG6) (Fuso Nerini et al., 2018). The target is still far from reached, in 2019 759 million people still lacked access to electricity in the world where the majority lives in Sub-Saharan Africa (IEA, IRENA, UNSD, World Bank, WHO, 2021).

Energy planning is central to achieve these goals, where energy systems optimization models (ESOMs) are important tools to explore different scenarios and give insight (Aryanpur et al., 2021; Pfenninger et al., 2014). To achieve SDG7 by 2030 decentralized energy supply options have been identified as central due to the given timeframe (IEA, IRENA, UNSD, World Bank, WHO, 2021). Energy system modelling frameworks, such TIMES from IEA-ETSAP are often applied with the assumption that the countries investigated already have a large grid infrastructure, and typically simplify spatial constraints associated with those that are unelectrified (IEA ETSAP, 2022). For countries with low electrification rates grid roll-out is often difficult and spatial characteristics are important with respect to electrification costs and technology choice.

With the energy transition to larger quantities of variable renewable energies and larger shares of distributed technologies, new challenges in energy modelling arise. Most decentralized supply options, such as solar and wind, are intermittent technologies which requires increased temporal resolution to understand the implications of it (Pfenninger et al., 2014).

At the same time with increasing decentralized supply options with variations of energy resources across the spatial dimension requires analysis with increased spatial resolution (Pfenninger et al., 2014). A recent review of ESOM by Plazas-Niño et al. (2022) highlights the need for higher spatial granularity in

ESOM to represent variable renewable energy resources better. Furthermore, the authors highlight the need for better representation of specific features in developing countries to allow specific representation of local challenges. Increasing the spatial resolution of energy modelling could allow investigation across three key dimensions. Socio-economic aspects, such as population demographics and income influence the spatial pattern of demand. Supply-side aspects, including the changing spatial pattern of renewable resources and location of transmission infrastructure. Demand-side aspects to identify local demand variations and regional consumer variations. Increasing the spatial resolution in energy systems optimization models often comes with a computational cost which can be motivated in an heterogenous system (Aryanpur et al., 2021).

Several models have been developed using Geospatial Information System (GIS) to address the rural electrification planning in terms of network, generation sizing and clustering demand cells (Ciller and Lumbreras, 2020). As an example Network planner (Kemausuor et al., 2014) and Open Source Spatial electrification Tool (OnSSET) (Korkovelos et al., 2019; Mentis et al., 2017) use different heuristic methods (minimum-spanning tree, Locality-Sensitive Hashing) to find the “best” technology choice and network solution for each location (such as village/house/cluster). Zeyringer et al. (2015) developed a spatially disaggregated MILP model for Kenya. It optimizes the cost of either extending the grid to a unelectrified cell or suppling off-grid PV technology instead. However, these models treat the grid as a black box. While a noteworthy initial effort limited itself to the study of a single village (Howells et al., 2005).

There are some studies that have soft-linked OnSSET with a long-term energy model (Open Source Energy Modelling System (OSeMOSYS)) which feeds back the grid cost (Moksnes et al., 2017; Pappis et al., 2021). A study by (Carvallo et al., 2017) investigates low carbon futures in Kenya for 47 load centres with a MILP model. However, they do not explicitly model unserved population nor include off-grid supply options. Demand side geospatial modelling is also explored in (Rocco et al., 2021) with an OSeMOSYS model for Tanzania with detailed demand projections following the Multi-Tier framework for households[1]. The resolution for the GIS analysis is 10x10 km in the pre-processing step but then aggregated to 6 demands in the optimization run. All these models account for grid in a detailed way, however the spatial dimension either uses approximate methods (OnSSET) or is modelled on an aggregated level.

For Uganda Trotter et al. (2019) developed a multi objective MILP model for Uganda for 112 different regions where the transmission and distribution network are integrated in the model allowing on-grid and off-grid electrification at different percentages. The work by Trotter et al. covers both the grid and a relatively high spatial resolution. The model does not account for variations within a year, but instead uses annual values in a multiyear approach.

In this paper we approach the rural electrification planning with long-term energy planning using linear programming. Linear programming (LP) computes: a globally optimal solution; allows easy exploration of trade-offs between supply; and demand as well as shadow prices. A large proportion of ESOMS adapt LP frameworks for this reason (Plazas-Niño et al., 2022). In our case, the additional programmed link for

the spatial data that is introduced into the model generation allows nimble and rapid exploration of computational trade-offs versus detail of insights. We focus on the problem related to the national planning of rural electrification planning (SDG 7.1, universal access to electricity) in the case of Kenya where still 16 million people lack access to electricity (World Bank, 2021). We define the following research questions for this study:

- How can a high spatial resolution be modelled in LP modelling tools such as OSeMOSYS?

- What is the cost and technology optimal solution for Kenya when optimizing with high spatial resolution in OSeMOSYS?

The paper is structured as follows, Methods in Section 2, Results in Section 3 and Discussion in Section 4 and Conclusions in Section 5.

[1] International Energy Agency and World Bank, Sustainable Energy for All 2013-2014: Global Tracking Framework Report, 2014.

2. Methods

2.1 Reproducible and FAIR data

The work has for transparency and reproducibility been developed with an open-source Python and GNU MathProg code, with open-access data where the workflow is reproducible from the GitHub and where needed, datasets are uploaded to Zenodo and follow the FAIR (Findable, Accessible, Interoperable and Reusable) principles (Wilkinson et al., 2016). The open-source GitHub workflow can be further enhanced by other users and allows to report and track *issues*. The data used to perform the analysis are listed in text files and all URL:s are also listed in the Appendix. The data is licensed under permissive licenses and are in formats that are interoperable such as csv and shapefiles.

2.2 Model description - GEOSeMOSYS

In this section we describe the general modelling steps that enable linking geospatial data with OSeMOSYS, *GEOSeMOSYS* [2]. The modelling is composed of a computational workflow of pre-processing steps in GIS which identify location-specific data.

We use OSeMOSYS as it enables us to model the central power plants simultaneously with the location specific data using a linear programming approach. OSeMOSYS is an open-source energy systems optimization model (Howells et al., 2011) which has been applied for numerous applications from large continental models to interlinkages in climate, land, energy and water nexus to mention a few (Gardumi et al., 2018).

The geospatial information is preserved in the optimization to be able to explore trade-offs between supply and demand across a country divided into a set of regions simultaneously. In most linear

programming environments, there is a limit to how many sets/indices you can define before the problem is not computationally possible to solve. Therefore, the geospatial and temporal data is aggregated to a lower spatial and temporal resolution for the optimization. While this creates simplifications, nonetheless, it provides insights. In this paper the low spatial resolution is referred to as *cells*. The higher resolution (1x1km) is referred to as *settlements*.

The geospatial processing is first handled in a higher resolution for three calculations:

1. estimating where the electrified population live,
2. estimate the distance of low voltage (LV) lines to un-electrified population,
3. socio-economic demand indicators,

The following subsections describe the general steps to build the OSeMOSYS data file and model file.

2.2.1 Estimate current electrified cells (1x1km resolution)

The initial step is to run an *electrification algorithm* (Mentis et al., 2017) which approximates which settlements that are electrified in the base year. Night-time light has been found to be a good proxy for identifying where households are electrified and not (Falchetta et al., 2019). In addition to night-time light, other datasets are considered such as distance to substations, low voltage (LV) lines, medium voltage (MV) lines, existing mini-grid.

In many cases the data availability is limited in developing countries, however some global datasets are available. The GIS data that is used for all GIS-processing in this paper is listed in Table 1. Some of the data is global, and some specific for Kenya. However, they can be changed to other regions specified by the user.

Table 1. GIS datasets in case application for Kenya

GIS datasets
Night-time lights (Elvidge et al., 2021)
Population (Facebook, 2021a)
Transmission network (KPLC, 2020a)
Roads (Jordan et al., 2021)
Mini-grid (Jordan et al., 2020)
Substations and transformers (KPLC, 2020b) (KPLC, 2017)
GDP PPP (Kummu et al., 2019)
Capacity factor wind (Staffell and Pfenninger, 2016)
Capacity factor PV (Pfenninger and Staffell, 2016)

2.2.2 Demand distributed to electrified/unelectrified cells

The demand cells are divided into two types, electrified $_{\text{in base year}}$ and un-electrified $_{\text{in base year}}$, to allow separate demand profiles and projections. This gives a more detailed view of the remote areas which are not connected to the grid in the base year. To approximate the electrified $_{\text{in base year}}$ demand for each demand cell the GDP PPP Figure 4(Kummu et al., 2019) and population is used as a proxy to distribute the demand. A higher GDP is assumed to have a higher energy activity, thus high GDP PPP will give a higher share of demand (Burke and Csereklyei, 2016). The equations are defined below in Equation 1 and Equation 2. Since a prioritization of which communities to connect first is not available, all unelectrified $_{\text{in base year}}$ cells are linearly electrified at the same time until 100% connectivity is achieved.

Equation 1. Electrified cells demand distribution

$$Electricity\ demand_{electrified\ cells} = \left(\frac{GDP_{XY_{demandcell}}}{GDP_{sum\ Kenya}} * 0.5 + \frac{Population_{XY_{demandcell}}}{Population_{sum\ elec}} * 0.5\right) \cdot demand_{elec}$$

Equation 2. Un-electrified cells demand distribution

$$Electricity\ demand_{un-electrified\ cells} = \frac{Population_{XY_{demandcell}}}{Population_{sum\ unelec}} \cdot demand_{unelec}$$

2.2.3 Transmission lines to un-electrified cells

An extension of the transmission line to unelectrified $_{\text{in base year}}$ cells is considered in the model. For cells that lack grid connection in the initial electrification analysis (e.g. are not electrified or are electrified by

mini-grid) the distance to extend transmission lines are calculated for nearby cells. Cells located further away than 50 km can only be connected by either an existing or newly electrified adjacent cell.

To enable the adjacent transmission lines to supply the next transmission line they are connected cell-by-cell in the model. This enables the model to expand to adjacent cells from the existing grid without having overlapping lines extended in parallel. In addition, nearby mini-grid cells can supply adjacent cells as they can supply the connecting transmission lines. One central aspect of the model set up is the energy flows which are described in the reference energy system (RES). The RES represents how the energy flows and are converted and transmitted through the energy system. In Figure 2 the transmission lines connections are illustrated. The pink cell is the unelectrified $_{\text{in base year}}$ cell closest to an electrified $_{\text{in base year}}$ cell and the central transmission grid can supply this cell at an installation cost/capacity unit.

2.2.4 Distribution lines to unelectrified cells (Pathfinder)

To identify the required distance of the new distribution lines to connect the unelectrified $_{\text{in base year}}$ settlements, an approximation using a greedy algorithm of many-to-many Dijkstra algorithm is applied. The original Dijkstra finds the shortest path between two points (Dijkstra, 1959) however, a network is not a two-point problem. The many-to-many Dijkstra algorithm was developed by Roher at Facebook (*Pathfinder*, 2019) and keeps the shortest path network in a heap queue. The Pathfinder algorithm takes three matrices as input: *origin*, *targets*, and *weights*. The origin is the starting point for the network. The targets are to be included in the network. The weights are the "cost" of travelling that route where a low weight is cheaper to follow and will many times be preferred. The Pathfinder algorithm has been applied to identify existing MV-lines where data availability is low (Arderne et al., 2020) with good accuracy (75%) compared to known existing MV-lines.

MV- and LV-lines follow roads due to logistical reasons, and therefore the weights are lower following the road (weight 0.5). Additionally, the current HV-, MV- and LV-lines are included since that is existing infrastructure (with weight 0.01). The remainder of the weights are set to 1. The targets in the algorithm are the unelectrified $_{\text{in base year}}$ settlements from the electrification algorithm. As the HV/MV transmission lines distance are cell specific (see section 2.2.3 Transmission lines to un-electrified cells) the Pathfinder algorithm is run individually for each cell to assure that the suggested distribution lines are not interlinked to the other cell (in case the optimal solution does not install distribution lines in neighbouring cell). This makes the suggested distribution lines a little bit longer than if they are optimized all in one network. The shortest path network distance is then reduced where there is overlap with the existing grid to avoid double counting. To account for additional distribution lines per 1x1km cell the gridded length from (van Ruijven et al., 2012) was adapted for the model and aggregated for an average for each cell (for details on equations see Appendix Equation 7-12).

2.2.5 Distribution lines in OSeMOSYS to unelectrified in base year

To respect the spatial dimension in OSeMOSYS, but at the same time allow varying cell size, we introduce a new variable *km* in the OSeMOSYS model which represents the new installed km. Within each cell the

maximum total km allowed is the estimated km from the Pathfinder estimation. The peak demand for unelectrified $_{\text{in base year}}$ cell is calculated per year and accounts for losses. The peak is then divided by the number of km calculated for the cell. The *Peakdemand* represents the unit peakcapacity/km and is defined as an exogenous parameter (for details see Appendix Equation 5, Equation 6). This gives a uniform peak load, which in case the full demand is met by distribution lines, will require to install all km (Equation 3). Equation 3 disjoins the km from capacity (as the PeakDemand increases proportional to the annual max peak) and the LV line cost can then be defined as the cost per km (Equation 4).

Equation 3

$$NewCapacityDistribution\{r\ in\ REGION, t\ in\ TECHNOLOGY, y\ in\ YEAR\}: Peakdemand[r,t,y] * (sum\{yy\ in\ YEAR: y - yy >= 0\}\ km[r,t,yy]) \geq TotalCapacityAnnual[r,t,y]$$

Equation 4

$$NetworkCostPerCapacitykm\{r\ in\ REGION, t\ in\ TECHNOLOGY, y\ in\ YEAR\}: km[r,t,y] * CapitalCostkmkW[r,t,y] = CapitalCostnetwork[r,t,y]$$

All parameters and equations added to OSeMOSYS can be found in the appendix and on the GitHub page for GEOSeMOSYS_Kenya.

2.3.6 Intermittent electricity generation and storage

For the solar and wind potential the hourly location specific data is retrieved from Renewables.ninja. The dataset from Renewables Ninja gives an hourly approximation for each location (Pfenninger and Staffell, 2016; Staffell and Pfenninger, 2016). The wind turbine used in the model is Vestas 42, for the time interval 1 January to 31 December 2016. For the Solar PV the tilt was set to 35 degrees and azimuth of 180^{o} [3] for all solar PV. The 2016 wind and solar profile is assumed to be representative for all years up to 2040 and not sensitive to climate change.

Batteries are included in the model with a simplified implementation for both wind power and PV. The battery is calculated hourly and supplying power when the capacity factor is 0. The batteries considered are both for residential and commercial implementation. For residential a battery with a 1 kW capacity and energy storage of 4 kWh[4]. For commercial a capacity 600 kW and 2400 kWh storage is considered for PV mini-grid with 8h storage (at 50% capacity factor) (Augustine and Blair, 2021). The round-trip efficiency (implemented as capacity factor in the model) is expected to be 0.85 for the whole duration and recharged at the next time the capacity factor is over 0.

The available off-grid technologies modelled are *mini-grid*: wind, diesel generator and PV (with battery) and *stand-alone*: PV (with and without battery). The solar, wind and diesel mini-grid options are designed with distribution extension to the demand sites (Appendix, Figure 15). All mini-grid are also connected to the adjacent cells and can act as a local supplier (as seen in Figure 2) at the cost of building the connecting MV line and new distribution lines.

2.3.7 Shadow price in linear programming

From a linear programming optimization, the *dual value* for each of the constraints in the model can be obtained. The dual value is the marginal change per one unit increase and is often called the *shadow price or marginal cost*. The shadow price represents the marginal cost of the modelled commodity, in this paper electricity (Loulou et al., 2016). This is not the same as the levelized cost of electricity (LCOE) which represents the net present cost of electricity generation for a technology over its lifetime. In contrast, the dual value includes all parameters (all technologies and fuels) that (the cost optimal) additional unit of electricity would cost for that specific demand. This information is very useful to understand the local costs under complex supply chains.

2.3 Case application - Kenya

We use Kenya as a case application for two reasons: first Kenya has still a large share of un-electrified population (~30%), second there are detailed open access geospatial data from which the model could build from. The modelled resolution of 40x40 km cells leads to 378 cells for the country. For Kenya we have applied the same discount rate as in the Least Cost Power Development Plan (LCPDP) at 12% (Energy and Petroleum Regulatory Authority (EPRA)Kenya et al., 2021). To be able to model seasonal changes in supply and the demand the model has 4 seasons (January-April, May-July, August-October, November-December) and 3 day-splits with a peak demand in the evening between 19-22. Detailed techno-economic data for power plants can be found in the Appendix in Table 4, Table 5 and Table 6.

2.3.1 Estimate current electrified cells (1x1km resolution)

In the case of Kenya the night-time light (with a value over 0.5) identifies 38% of the population as electrified in combination with the High-Resolution Settlement Layer (HRSL) (Facebook, 2021a). To identify the remainder of the electrified households (70%) (World Bank, 2021) additional parameters such as mini-grid and transmission networks are added to the electrification algorithm. As seen in Figure 3 the estimated electrified population are centred around the south-/southwest of the country.

2.3.2 Demand distributed to electrified/unelectrified cells

Based on the electrification algorithm a total of 591 electrified $_{\text{in base year}}$ and unelectrified $_{\text{in base year}}$ *demand cells* are identified in Kenya. The total demand in the model follows the overall projected demand from the *Updated Least Cost Power Development Plan 2020-2040* reference and vision scenario (LCPDP 2020-2040) (Energy and Petroleum Regulatory Authority (EPRA)Kenya et al., 2021). We give unelectrified households a demand and demand profile, that is unmet until those households are electrified. Data for those households are calibrated in the base year. For the unelectrified $_{\text{in base year}}$ the reference demand follows the estimated rural demand from LCPDP of 78 kWh/connection. However, the *High demand* scenario for unelectrified $_{\text{in base year}}$ the demand is increased significantly to 1000 kWh/connection to juxtapose the technology choice for unelectrified $_{\text{in base year}}$ cells in GEOSeMOSYS. To still be able to compare the results to the Vision scenario from the LCPDP 2020-2040 the unelectrified $_{\text{in base year}}$ demand

is deducted from the overall projected demand. This means that the electrified $_{\text{in base year}}$ demand is lower than projected from the government for this scenario (Figure 4).

The demand profile for the electrified $_{\text{in base year}}$ (217) demand cells are assumed to have the same profile as the half hourly demand profile for Kenya as a whole in 2015 (KPLC, 2015). The initial demand profile for the unelectrified $_{\text{in base year}}$ demand cells is assumed to not be the same as the grid connected. Such a rural demand profile is not readily available for Kenya. However, a study from Tanzania on rural microgrid smart meter is assumed where Williams et al. analyse different customer segments in microgrids (2018). To be able to depict an average rural customer all types (home/business/public premises) are joint to one rural/unelectrified $_{\text{in base year}}$ demand profile in the model. As seen in Figure 5 the unelectrified $_{\text{in base year}}$ demand profile has a clear peak in the evening whereas the electrified $_{\text{in base year}}$ demand has a slightly lower peak with a flatter demand over the day. It is however expected that the demand profile will flatten when more electricity is consumed and the unelectrified $_{\text{in base year}}$ will also in the model transition to the same as electrified $_{\text{in base year}}$ demand profile.

2.3.3 Transmission lines to un-electrified cells

For Kenya 656 transmission lines between unelectrified $_{\text{in base year}}$ cells are assessed in the optimization. The relation between cost and capacity is assumed to be linear in the model. The transmission cost per MW-km is set to 3300 USD and in addition the substation is set to 24000 USD/MW (IEA, 2014). The cost of transmission line is multiplied with the length of each line. The transmission losses are 4.5% in base year and decreases to 3.5% in 2025. Distribution losses are modelled at 17% for the whole modelling period (Energy and Petroleum Regulatory Authority (EPRA)Kenya et al., 2021).

2.3.4 Distribution lines to un-electrified cells (Pathfinder)

The total distance for Pathfinder amounts for Kenya to 129,790 km (disregarding traversing distances). Accounting for the average needed length within each settlement the total length of the distribution lines to connect all unelectrified $_{\text{in base year}}$ cells amounts to 328,392 km. The current length of distribution lines in Kenya is 76,319 km (11 kV and 33 kV in 2020)(Energy and Petroleum Regulatory Authority (EPRA)Kenya et al., 2021). As was shown in Figure 3 the estimated electrified settlements in base year are centred around the mid and western parts of Kenya. The remaining un-electrified “targets” are much more sparsely situated as seen in Figure 6. For the additional length of the LV lines per cell the average length ranges between 0.44 km – 11 km [5], which is then multiplied with the estimated network length from Pathfinder.

2.3.7 Intermittent electricity generation and storage

To capture learning curves the projected costs are from NREL Annual Technology Baseline (ATB) (2021a). However, the overall battery cost considered in the ATB considers the labour cost in U.S. As the labour cost is not as high in Kenya the labour cost is reduced for residential batteries as it represents a very large

share of the total cost. According to the Global Wage report 2021-2021 (International Labour Organization, 2020) the ratio between the highest minimum wage in Kenya compared to U.S was approx. 0.11. Therefore, the *labour cost* in the ATB forecast, for residential batteries, is reduced by that factor. Similarly, the rent and building cost was assumed to have the same proportional reduction as labour.

The scenarios that are explored in this paper are harmonized with the demand projections from the Kenyan government. Demand is a key driver for cost and technology choice and therefore the different levels are important to assess (Moksnes et al., 2019). In addition, the Kenyan government has estimated a dry hydro scenario where the hydro power availability is affected by climate change (Energy and Petroleum Regulatory Authority (EPRA)Kenya et al., 2021). In the following table a summary of the scenarios is described.

Table 2. Scenario description

Scenario	
Reference	The demand follows the reference demand from LCPDP 2020-2040. The unelectrified $_{\text{in base}}$ year/rural demand is estimated in LCPDP to 78 kWh/connection with an annual growth of 4%. The household size is 4 people. With these low demands the annual rural demand amounts to 3% in 2030 of the total demand (Energy and Petroleum Regulatory Authority (EPRA)Kenya et al., 2021). Universal access to electricity is achieved in 2030. As the demand is lower for this scenario the unelectrified $_{\text{in base year}}$ demand profile is expected to move towards the flatter demand profile in 2030 as more appliances are introduced. The renewable technology costs are expected to decrease over time due to learning curves. The projections follow (NREL (National Renewable Energy Laboratory), 2021a) projections for moderate development.
High demand	The overall demand follows the Vision 2030 demand from LCPDP 2020-2040. However, the unelectrified $_{\text{in base year}}$ demand is modelled at 1000 kWh/connection with 6% annual growth. The household size is 4 people per household. With the demand of 1000 kWh/connection the rural demand amounts to 34% of the total demand in 2030. Universal access to electricity is achieved in 2030. As the demand is higher for this scenario the unelectrified $_{\text{in bae year}}$ demand profile is expected to move towards the flatter demand profile in 2025 as more appliances are introduced. The renewable technology costs are expected to decrease over time due to learning curves. The projections follow (NREL (National Renewable Energy Laboratory), 2021a) projections for advanced development.
Dry	This scenario follows the same scenario settings as the High demand scenario; however, all hydropower is expected to decrease in production due to climate change. This is modelled from 2024 and onwards with reductions which range from -33% to -37% depending on the powerplant (Energy and Petroleum Regulatory Authority (EPRA)Kenya et al., 2021). Mini-grid diesel generator is not a technology option in this scenario.

2.4 Computational requirements

The detailed demand curve combined with geographical information and many decentralized technologies leads to a large linear programming model which consists of 3812 technologies and 977 fuels. To be able to optimize the model IBM CPLEX was used, however other open-source solvers are available and could serve as options. The model however requires around 100 GB RAM to optimize if the

variable ProductionByTechnologyAnnual is included. The optimization takes ~5-8 hours in total. If ProductionByTechnologyAnnual is omitted, then it can be optimized on 32 GB RAM computer. The variable ProductionByTechnologyAnnual can be obtained with post-processing the output variables.
[2] https://github.com/KTH-dESA/GEOSeMOSYS_Kenya
[3] Azimuth angle = 180^0 (i.e., south-facing panels) for farms in the northern hemisphere. Kenya is situated on the equator, both north and south hemisphere.
[4] Total System Cost ($) Battery = Battery Storage Capacity (kWh) * Battery Energy Cost ($/kWh) + Battery Power Capacity (kW) * Battery Power Cost ($/kW) + Battery Power Constant ($)
[5] With a peak demand of 200W/connections, max capacity of the LV line to 10kW, and an inhibited area of 0.3 across all cells and scenarios.

3. Results

In this section the results from the modelled scenarios for the case application for Kenya are described with respect to the electricity generation, costs, emissions and capacities.

3.1 The role of demand

For the unelectrified $_{\text{in base year}}$ in the reference scenario most of the newly electrified demand (99% in reference scenario) is met by residential PV with batteries. An expansion of the connecting transmission lines in the northern parts is seen however only to already electrified $_{\text{in base year}}$ cells where the distribution network to the households exists. In Figure 7 the expansion of the transmission lines is displayed for 2025, 2030 and 2035 in combination with the installed distribution lines. The energy flow in the connecting transmission lines ranges from 5 GJ – 3391 GJ.

For the high demand scenario, the supply options are instead the opposite with 87% of the unelectrified $_{\text{in base year}}$ demand supplied by either mini grid and/or grid. The higher demand with high evening peaks leads to more diversified supply options. As seen in Figure 8 the distribution lines are installed already in 2025 for most of the cells. It is observed both where existing transmission lines are already installed in the base year and new extension with transmission lines to adjacent cells. The transmitted electricity range between 1-504,308 GJ.

Looking at the installed capacity of powerplants, mini-grid and stand-alone technologies for the different scenarios the new generation capacity for the reference case amounts to 7.5 GW which is slightly higher than in LCPDP 2020-2040 (which amounted to 5.717 GW) (Energy and Petroleum Regulatory Authority (EPRA)Kenya et al., 2021). As the LCPDP might have a different demand profile a discrepancy is expected. For the high demand and dry scenario the new capacity amounted to 15.8 GW resp. 15.9 GW compared to 14.5 GW in LCPDP Vision scenario (Energy and Petroleum Regulatory Authority (EPRA)Kenya et al., 2021).

Comparing the electricity production between the different scenarios, as seen in Figure 9, the predominant technology choice is geothermal for all scenarios. The coal power plant in Lamu is not fully utilized in the reference scenario starting at 4% capacity factor in 2027 and increasing to ~60% in the end of modelling period. For the dry scenario a decrease of the hydro power is observed already in 2025 compared to the high demand scenario. The decreased hydro power production is replaced by natural gas, coal, thermal power plants and distributed technologies.

3.2 Investment costs and local shadow prices

The total discounted costs in the reference scenario amounts to 6,940 million USD (period 2020-2040). The same scenario is estimated to amount to 10,055.1 million USD for the same time period in LCPDP (Energy and Petroleum Regulatory Authority (EPRA)Kenya et al., 2021). In LCPDP a reserve margin of ~19% is included which is not included in the scenarios for the case application. In addition, the discounted salvage value is deducted from the overall cost, which might not be the case in the LCPDP. The cost structure (in Figure 10) is for the largest share for power plans followed by stand-alone. The high demand scenario total discounted cost amounts to 12,102 MUSD and dry scenario total discounted cost amounts to 12,559 MUSD for the same period. The cost structure for the high demand scenario is also predominantly for power plants followed by extending the distribution lines.

Looking at the weighted annual average shadow price in the reference case a few patterns appear. The first pattern is that in the initial year of 2025 the shadow price is generally higher than in the year 2030 (ranging between 2.5 to 25 cent/kWh undiscounted) and then decreases to 0 to 5 cent/kWh. As the demand profile for unelectrified $_{\text{in base year}}$ has a very high evening peak in the reference case in 2025 and almost all the demand is supplied by PV with batteries the shadow price is exacerbated. The shadow price is zero for all time slices in 2025 except for the evening peak for November-December. In practice that indicates that all other months and times of the year there is an oversupply compared to the modelled demand. This is also what can be observed in 2030 for the unelectrified $_{\text{in base year}}$ when the demand profile converges to a flatter demand curve and the evening peak is covered by previous capacity installation the median shadow price is zero. For the electrified $_{\text{in base year}}$ the cost is more stable with slightly increasing costs over time when moving up the supply curve.

Comparing the shadow prices for the high demand and dry scenario, both scenarios has already in 2025 a large interquartile range. This illustrates the plethora of supplying technologies which was not observed in the reference scenario. The dry scenario does not have the option to install diesel generators, and at the same time the hydro power plants are decreasing their production due to dryer climate. This leads to larger shares of PV with batteries in the dry scenario for unelectrified $_{\text{in base year}}$ in combination with higher production of natural gas for the central power supply. In contrast in 2030, the shadow prices for unelectrified $_{\text{in base year}}$ in the high demand scenario shows a larger interquartile range with a median around 5 cent/kWh compared to the dry scenario with a median around 6 cent/kWh. For the high demand scenario, wind mini-grid is introduced at larger scale in 2030 which has varying capacity factors over the country. In the dry scenario the reduced hydro power is replaced by heavy fuel oil power plants and

transmission lines. For the dry scenario in 2035 wind mini-grid is also introduced in larger scale increasing the interquartile range. The outlier in both scenarios shows the diversity of supply options of in these scenarios such as PV with batteries mini-grid, PV stand alone and the range that the increasing demand has for the different cells.

3.2 CO2 emissions

Kenya has in their Nationally Determined Contribution (NDC) to the Paris agreement promised a reduction of 30% compared to Business as usual which is equal to a total of 100 MtCO2e for all sectors. Considering that the electricity sector has close to zero emissions in the base year and the other sectors emissions are expected to increase the electricity sector needs to be kept at low emissions to meet the NDCs (Ministry of Energy Kenya, 2018). As seen in Figure 13 the emissions start at around 0.3 MtCO2 and steadily increases to a maximum of 2.3 MtCO2 in reference and over 2.5 MtCO2 for high demand and dry scenario. The Lamu coal plant is installed in 2027 which has larger shares of production in the high demand and dry scenario which emits more CO2. In the LCPDP 2017-2037 (as the emissions are not reported in the 2020-2040 report) the reference case amounted to 0.3 MtCO2 in 2030 and the Vision scenario to 4 MtCO2 in 2030.

4. Discussion

In this paper we have explored how to increase both the spatial and temporal resolution in an energy systems optimization model for energy access. We used Kenya as case application and show that disaggregated demand leads to mostly off-grid connections in reference scenario, however with the high demand scenario almost all demand was connected to mini-grid/grid. Other studies have shown similar results where low demand in a spatial disaggregated models lead to more off-grid solutions while higher demand leads to more mini-grid/grid connections (Korkovelos et al., 2019; Mentis et al., 2017; Moksnes et al., 2017). In the reference scenario the results showed increased shares of variable renewables, supplied as distributed technologies. This is confirmed in the review by Aryanpur et al. (2021) which also found that increasing the spatial resolution leads to higher shares of variable renewable technologies. The shadow prices for Kenya gave insight on what one more unit of electricity for each of the 591 cells would cost. The range was quite large in the scenarios ranging between 0-25 cents per kWh. This raises questions about affordability when the shadow price is high. What was observed was that the trade-off between supply and demand was very clear, especially when the supply technology choice was PV with battery with a sharp evening peak in the reference scenario. The service level required for the PV with battery was high and lead to higher capacity with zero shadow price in all other time slices than November-December evening peak. At the same time, it could be observed that the decreasing hydro power did not affect the results much overall in cost or electricity generation.

The methods of GEOSeMOSYS are applicable not only for Kenya but for studies that wants to understand technology choices for energy access in combine with the grid supplied power plants. Important key spatial aspects are captured in the spatially disaggregated model which a “one node”

model cannot capture. First, the trade-off between supply and demand in a location specific context provide insight on required service level. The shadow price is an output from linear programming which can give further insight on the marginal cost for the service level in a complex energy system. Second, the model handles both the central power plants, expansion of the transmission and distribution lines and distributed technologies in one multi-year model. Third, the model is built with open-access data and open-source code. The open-source code can be further enhanced by other users, and issues reported to further improve the workflow. The chosen spatial resolution leads to a large number of technologies and fuels. However, the model can be solved on a desktop computer with 32 GB RAM if the fast version of OSeMOSYS is used. Post-processing is then needed to calculate some of the results. Open-source solvers are available such as CBC which can be used instead of CPLEX, which is only free on an academic license. The model generation code is also largely programmed in Python and the spatial resolution is flexible, so it is possible to reduce the number of cells and run a lower resolution on a desktop computer. Fourth, the spatial dimension is better captured with the Pathfinder to estimate the required distribution lines to unelectrified, which is a slightly different application than previous version which looks to estimate the existing MV-network (Arderne et al., 2020). This in combination with the equation in OSeMOSYS allowing for incremental km installation for distribution lines supplying the final demand allows for increased spatial analysis in a linear programming model.

However, several key parameters in the model have a high uncertainty. The electrification algorithm from which estimations on where the electrified and un-electrified population live which forms the model basis. This estimation is difficult to validate and is central to the remainder of the calculations. A study by (Falchetta et al., 2019) found that, compared to the available census from the studies countries, night-time light is broadly a good parameter to approximate electrified population. In our study we included several more parameters from the electricity infrastructure (e.g. transmission lines, substations, transformers) where distance to road, transformers and LV lines were the main parameters in combination with night-time lights (and a detailed breakdown of the decision criterions for electrifying a cell can be seen in appendix in Figure 18). All the spatial data is located in the centre of the cell meaning that the solar/wind capacity factor and grid extension is to the centre of the cell. As the cells are coarse better and worse conditions would certainly exist within the cell. In addition, the reserve margin is not included as the computational time increases dramatically when modelling with high spatial granularity.

Looking at the expansion of the transmission lines between the cells is modelled at 3300 USD/MW-km, with no lower limit. In addition is the cost applied in both directions. This leads to transmission lines being installed at very low capacities at low cost per km. The OSeMOSYS distribution equations works for the final technology supplying the demand as the peak demand is linear to the distribution lines in those cases. The transmission lines are however more complex, supplying adjacent cells with multiple demands downstream. Therefore, the same equations cannot be transferred upstream with the current formulation. In linear programming the optimal results can install very small capacity/km per technology, which might be unlikely when planning the electricity system. One way to mitigate this is to add a lower limit and optimize a Mixed Integer Linear program (MILP). However, the computational time increases dramatically, which was undesirable in this study. Finally, the double distribution lines, one supplying

from the grid and the other suppling from mini-grid, in cells that have transmission lines in the base year leads to higher costs as the distribution lines cannot be used intertwined.

5. Conclusions

We have in this paper modelled an energy optimization model with a high spatial and medium temporal resolution with an open-source model generation code and OSeMOSYS, GEOSeMOSYS. Many energy systems models capture medium to long term temporal investment dynamics but represent spatial realities poorly. While many spatially explicit models do not capture said medium to long-term system-wide dynamics. In our modelling, we capture elements of both simultaneously.

Several key methods have been developed and largely automated in Python.

The proposed workflow:

- estimates where the electrified population lives,
- considers socio-economic aspects for demand estimation,
- accounts for different demand profiles for electrified $_{\text{in base year}}$ and unelectrified $_{\text{in base year}}$.
- estimates the length of new distribution lines to unelectrified $_{\text{in base year}}$,
- allows connecting adjacent cells with transmission lines in the optimization run to expand the grid/mini-grid,
- additional equations are added to the distribution lines in the OSeMOSYS model code to enable the distribution lines to be accounted for per km.

All these building blocks are then connected to the corresponding parameters in OSeMOSYS and optimized in one model. The spatial computations that allow for a better spatial representation that has been developed for this paper are the distribution equations for OSeMOSYS model modification. These decouple the capacity from the km estimation. Furthermore, is the application of Pathfinder slightly different, connecting population which are un-electrified, than previous application (Arderne et al., 2020) which estimates the existing MV-lines.

For our case application we find that for Kenya the cost optimal solution is mainly distributed technologies to unelectrified $_{\text{in base year}}$ for lower demand, however when supplying a high demand, the shift is clear to more grid and mini-grid supply to the unelectrified $_{\text{in base year}}$. The overall cost structure for the reference scenario has a larger share of standalone compared to the high demand scenario which instead has a larger share to distribution. However, most of the costs are in both scenarios from power plants. From the shadow prices we could see a variation over time and if the demand was supplied to an unelectrified $_{\text{in base year}}$ or not. The cost increased in combination with a sharp evening peak when supplied by stand-alone systems. There where it's possible to reduce the peaky profile of new connections

the economics of stand-alone systems would be improved (as peak marginal costs would reduce). That might include integrating very high-efficiency appliances; encouraging changes in appliance time of use; or improving storage (this could be electrical, thermal, or chemical - depending on the service that is being demanded at peak).

Future work

The spatial resolution was in this study chosen at a level where the computational time did not exceed 10h. As Khavari et al. (2021) highlights the results in OnSSET change with different population aggregations. This indicates that it would be of value to also investigate different spatial resolutions further in combination with the temporal resolution for OSeMOSYS to understand the changes in results.

The battery for off-grid technologies is implemented using a simplified calculation using the capacity factors. If storage calculations were implemented the battery would potentially be more efficiently used.

The current GitHub repository code is specifically developed for Kenya; however, the code can be of interest for other energy modellers and can be modified to be more general. This would not require a huge effort as much of the code is already based on the GIS data provided by the user.

Declarations

Competing interests: The authors declare no competing interests.

Author contribution (CRediT)

Nandi Moksnes: Conceptualization, Methodology, Software, Validation, Formal analysis, Investigation, Resources, Data Curation, Writing - Original Draft, Visualization, Project administration.

Mark Howells: Conceptualization, Methodology, Validation, Writing - Review & Editing, Supervision.

William Usher: Methodology, Validation, Writing - Review & Editing, Supervision.

Acknowledgement

The computations for the optimization were performed on resources provided by the Swedish National Infrastructure for Computing (SNIC) at PDC Center for High Performance Computing at KTH Royal Institute of Technology. Jiang Gong at PDC is acknowledged for assistance concerning technical and implementation aspects in making the code run on Tegnér and Dardel (PDC). We furthermore acknowledge Alexandros Korkovelos for his valuable comments to further improve selected GIS aspects, Jagruti Thakur for her valuable comments in respect to the modelling setup and Babak Khavari for support on general GIS questions. Howells acknowledges supplementary funding support from the

Climate Compatible Growth (CCG) programme of the UKs Forign, Commonwealth and Development Office (FCDO). The views expressed in this paper are not necessarily reflect those of the FCDO.

References

Arderne, C., Zorn, C., Nicolas, C., Koks, E.E., 2020. Predictive mapping of the global power system using open data. Sci Data 7, 19. https://doi.org/10.1038/s41597-019-0347-4

Aryanpur, V., O'Gallachoir, B., Dai, H., Chen, W., Glynn, J., 2021. A review of spatial resolution and regionalisation in national-scale energy systems optimisation models. Energy Strategy Reviews 37, 100702. https://doi.org/10.1016/j.esr.2021.100702

Augustine, C., Blair, N., 2021. Storage Futures Study: Storage Technology Modeling Input Data Report (No. NREL/TP-5700-78694, 1785959, MainId:32611). https://doi.org/10.2172/1785959

Burke, P.J., Csereklyei, Z., 2016. Understanding the energy-GDP elasticity: A sectoral approach. Energy Economics 58, 199–210. https://doi.org/10.1016/j.eneco.2016.07.004

Carvallo, J.-P., Shaw, B.J., Avila, N.I., Kammen, D.M., 2017. Sustainable Low-Carbon Expansion for the Power Sector of an Emerging Economy: The Case of Kenya. Environ. Sci. Technol. 51, 10232–10242. https://doi.org/10.1021/acs.est.7b00345

Ciller, P., Lumbreras, S., 2020. Electricity for all: The contribution of large-scale planning tools to the energy-access problem. Renewable and Sustainable Energy Reviews 120, 109624. https://doi.org/10.1016/j.rser.2019.109624

Dijkstra, E.W., 1959. A Note on Two Problemsin Connexionwith Graphs. Numerische Mathematlk 269–27 I.

Elvidge, C.D., Zhizhin, M., Ghosh, T., Hsu, F.-C., Taneja, J., 2021. Annual Time Series of Global VIIRS Nighttime Lights Derived from Monthly Averages: 2012 to 2019. Remote Sensing 13, 922. https://doi.org/10.3390/rs13050922

Energy and Petroleum Regulatory Authority (EPRA)Kenya, Geothermal Development Company, KenGen, Kenya Power, Rural electrification and renewable energy corporation, KETRACO, Nuclear Power and Energy Agency, 2021. Updated least cost power development plan Study period 2020-2040.

Facebook, 2021a. Kenya: High Resolution Population Density Maps - Humanitarian Data Exchange [WWW Document]. URL https://data.humdata.org/dataset/highresolutionpopulationdensitymaps-ken (accessed 9.27.21).

Facebook, 2021b. Kenya: High Resolution Population Density Maps - Humanitarian Data Exchange [WWW Document]. URL https://data.humdata.org/dataset/highresolutionpopulationdensitymaps-ken (accessed 9.27.21).

Falchetta, G., Pachauri, S., Parkinson, S., Byers, E., 2019. A high-resolution gridded dataset to assess electrification in sub-Saharan Africa. Scientific Data 6. https://doi.org/10.1038/s41597-019-0122-6

Fuso Nerini, F., Tomei, J., To, L.S., Bisaga, I., Parikh, P., Black, M., Borrion, A., Spataru, C., Castán Broto, V., Anandarajah, G., Milligan, B., Mulugetta, Y., 2018. Mapping synergies and trade-offs between energy and the Sustainable Development Goals. Nature Energy 3, 10–15. https://doi.org/10.1038/s41560-017-0036-5

GADM, 2021. GADM [WWW Document]. URL https://gadm.org/download_country_v3.html (accessed 2.27.21).

Gardumi, F., Shivakumar, A., Morrison, R., Taliotis, C., Broad, O., Beltramo, A., Sridharan, V., Howells, M., Hörsch, J., Niet, T., Almulla, Y., Ramos, E., Burandt, T., Balderrama, G.P., Pinto de Moura, G.N., Zepeda, E., Alfstad, T., 2018. From the development of an open-source energy modelling tool to its application and the creation of communities of practice: The example of OSeMOSYS. Energy Strategy Reviews 20, 209–228. https://doi.org/10.1016/j.esr.2018.03.005

Gioutsos, D.M., Blok, K., van Velzen, L., Moorman, S., 2018. Cost-optimal electricity systems with increasing renewable energy penetration for islands across the globe. Applied Energy 226, 437–449. https://doi.org/10.1016/j.apenergy.2018.05.108

Howells, M., Rogner, H., Strachan, N., Heaps, C., Huntington, H., Kypreos, S., Hughes, A., Silveira, S., DeCarolis, J., Bazillian, M., Roehrl, A., 2011. OSeMOSYS: The Open Source Energy Modeling System. Energy Policy 39, 5850–5870. https://doi.org/10.1016/j.enpol.2011.06.033

Howells, M.I., Alfstad, T., Victor, D.G., Goldstein, G., Remme, U., 2005. A model of household energy services in a low-income rural African village. Energy Policy 33, 1833–1851. https://doi.org/10.1016/j.enpol.2004.02.019

IEA, 2019. WORLD ENERGY OUTLOOK 2019. OECD Publishing 810. https://doi.org/10.1787/caf32f3b-en

IEA, 2014. Electricity Transmission and Distribution - ETSAP [WWW Document]. URL https://iea-etsap.org/E-TechDS/PDF/E12_el-t&d_KV_Apr2014_GSOK.pdf (accessed 10.18.21).

IEA ETSAP, 2022. IEA-ETSAP | Times [WWW Document]. TIMES. URL https://iea-etsap.org/index.php/etsap-tools/model-generators/times (accessed 5.24.22).

IEA, IRENA, UNSD, World Bank, WHO, 2021. Tracking SDG 7: The Energy Progress Report. World Bank, Washington DC.

International Labour Organization, 2020. Global Wage Report 2020–21. Wages and minimum wages in the time of COVID-19 (No. ISBN 978-92-2-031945-1). Geneva: ILO,.

Jakhrani, A.Q., Othman, A.-K., Rigit, A.R.H., Samo, S.R., 2012. Estimation of carbon footprints from diesel generator emissions, in: 2012 International Conference on Green and Ubiquitous Technology. Presented at the 2012 International Conference on Green and Ubiquitous Technology (GUT), IEEE, Jakarta, pp. 78–81. https://doi.org/10.1109/GUT.2012.6344193

Jordan, A.R., Balla;, P., Njagi;, L., Banerjee, S., 2021. Kenya - Roads - ENERGYDATA.INFO [WWW Document]. URL https://energydata.info/dataset/kenya-roads-1 (accessed 6.8.21).

Jordan, A.R., Balla;, P., Njagi;, L., Banerjee, S., 2020. Kenya - Overview of Off-grid Electricity Service Areas - ENERGYDATA.INFO [WWW Document]. URL https://energydata.info/dataset/kenya-overview-of-off-grid-electricity-service-areas (accessed 6.8.21).

Kemausuor, F., Adkins, E., Adu-Poku, I., Brew-Hammond, A., Modi, V., 2014. Electrification planning using Network Planner tool: The case of Ghana. Energy for Sustainable Development 19, 92–101. https://doi.org/10.1016/j.esd.2013.12.009

Khavari, B., Sahlberg, A., Usher, W., Korkovelos, A., Fuso Nerini, F., 2021. The effects of population aggregation in geospatial electrification planning. Energy Strategy Reviews 38, 100752. https://doi.org/10.1016/j.esr.2021.100752

Korkovelos, A., Khavari, B., Sahlberg, A., Howells, M., Arderne, C., 2019. The Role of Open Access Data in Geospatial Electrification Planning and the Achievement of SDG7. An OnSSET-Based Case Study for Malawi. Energies 12, 1395. https://doi.org/10.3390/en12071395

KPLC, 2020a. Kenya - Kenya Electricity Network - ENERGYDATA.INFO [WWW Document]. URL https://energydata.info/dataset/kenya-kenya-electricity-network (accessed 6.8.21).

KPLC, 2020b. Kenya - Primary Substations - ENERGYDATA.INFO [WWW Document]. URL https://energydata.info/dataset/kenya-primary-substations (accessed 6.8.21).

KPLC, 2020c. Kenya - Kenya Electricity Network - ENERGYDATA.INFO [WWW Document]. URL https://energydata.info/dataset/kenya-kenya-electricity-network (accessed 6.8.21).

KPLC, 2017. Kenya - Distribution Transformers - ENERGYDATA.INFO [WWW Document]. URL https://energydata.info/dataset/kenya-distribution-transformers (accessed 6.8.21).

KPLC, 2015. Half-hourly load profile 2015.

Kummu, M., Taka, M., Guillaume, J.H.A., 2019. Data from: Gridded global datasets for Gross Domestic Product and Human Development Index over 1990-2015. https://doi.org/10.5061/DRYAD.DK1J0

Loulou, R., Goldstein, G., Kanudia, A., Lettila, A., Remme, U., 2016. Documentation for the TIMES Model.

Mentis, D., Howells, M., Rogner, H., Korkovelos, A., Arderne, C., Zepeda, E., Siyal, S., Taliotis, C., Bazilian, M., de Roo, A., Tanvez, Y., Oudalov, A., Scholtz, E., 2017. Lighting the World: the first application of an open source, spatial electrification tool (OnSSET) on Sub-Saharan Africa. Environmental Research Letters 12, 085003. https://doi.org/10.1088/1748-9326/aa7b29

Ministry of Energy Kenya, 2018. Updated Least Cost Power Development Plan 2017-2037 [WWW Document]. URL http://gak.co.ke/wp-content/uploads/2019/02/Updated-Least-Cost-Power-Development-Plan-2017-2022-min.pdf (accessed 4.7.21).

Moksnes, N., 2016. UN Sustainable development goals from a Climate Land Energy and Water perspective for Kenya (MSc). KTH, Stockholm.

Moksnes, N., Korkovelos, A., Mentis, D., Howells, M., 2017. Electrification pathways for Kenya–linking spatial electrification analysis and medium to long term energy planning. Environmental Research Letters 12, 095008. https://doi.org/10.1088/1748-9326/aa7e18

Moksnes, N., Rozenberg, J., Broad, O., Taliotis, C., Howells, M., Rogner, H., 2019. Determinants of energy futures—a scenario discovery method applied to cost and carbon emission futures for South American electricity infrastructure. Environmental Research Communications 1, 025001. https://doi.org/10.1088/2515-7620/ab06de

NREL (National Renewable Energy Laboratory), 2021a. Annual Technology Baseline. Golden, CO: National Renewable Energy Laboratory.

NREL (National Renewable Energy Laboratory), 2021b. Useful Life [WWW Document]. URL https://www.nrel.gov/analysis/tech-footprint.html (accessed 2.18.22).

Pappis, I., Sahlberg, A., Walle, T., Broad, O., Eludoyin, E., Howells, M., Usher, W., 2021. Influence of Electrification Pathways in the Electricity Sector of Ethiopia—Policy Implications Linking Spatial Electrification Analysis and Medium to Long-Term Energy Planning. Energies 14, 1209. https://doi.org/10.3390/en14041209

Pathfinder, 2019. . Facebook Research.

Pfenninger, S., Hawkes, A., Keirstead, J., 2014. Energy systems modeling for twenty-first century energy challenges. Renewable and Sustainable Energy Reviews 33, 74–86. https://doi.org/10.1016/j.rser.2014.02.003

Pfenninger, S., Staffell, I., 2016. Long-term patterns of European PV output using 30 years of validated hourly reanalysis and satellite data. Energy 114, 1251–1265. https://doi.org/10.1016/j.energy.2016.08.060

Plazas-Niño, F.A., Ortiz-Pimiento, N.R., Montes-Páez, E.G., 2022. National energy system optimization modelling for decarbonization pathways analysis: A systematic literature review. Renewable and

Sustainable Energy Reviews 162, 112406. https://doi.org/10.1016/j.rser.2022.112406

Rocco, M.V., Fumagalli, E., Vigone, C., Miserocchi, A., Colombo, E., 2021. Enhancing energy models with geo-spatial data for the analysis of future electrification pathways: The case of Tanzania. Energy Strategy Reviews 34, 100614. https://doi.org/10.1016/j.esr.2020.100614

Staffell, I., Pfenninger, S., 2016. Using bias-corrected reanalysis to simulate current and future wind power output. Energy 114, 1224–1239. https://doi.org/10.1016/j.energy.2016.08.068

Trotter, P.A., Cooper, N.J., Wilson, P.R., 2019. A multi-criteria, long-term energy planning optimisation model with integrated on-grid and off-grid electrification – The case of Uganda. Applied Energy 243, 288–312. https://doi.org/10.1016/j.apenergy.2019.03.178

van Ruijven, B.J., Schers, J., van Vuuren, D.P., 2012. Model-based scenarios for rural electrification in developing countries. Energy 38, 386–397. https://doi.org/10.1016/j.energy.2011.11.037

Wilkinson, M.D., Dumontier, M., Aalbersberg, Ij.J., Appleton, G., Axton, M., Baak, A., Blomberg, N., Boiten, J.-W., da Silva Santos, L.B., Bourne, P.E., Bouwman, J., Brookes, A.J., Clark, T., Crosas, M., Dillo, I., Dumon, O., Edmunds, S., Evelo, C.T., Finkers, R., Gonzalez-Beltran, A., Gray, A.J.G., Groth, P., Goble, C., Grethe, J.S., Heringa, J., 't Hoen, P.A.C., Hooft, R., Kuhn, T., Kok, R., Kok, J., Lusher, S.J., Martone, M.E., Mons, A., Packer, A.L., Persson, B., Rocca-Serra, P., Roos, M., van Schaik, R., Sansone, S.-A., Schultes, E., Sengstag, T., Slater, T., Strawn, G., Swertz, M.A., Thompson, M., van der Lei, J., van Mulligen, E., Velterop, J., Waagmeester, A., Wittenburg, P., Wolstencroft, K., Zhao, J., Mons, B., 2016. The FAIR Guiding Principles for scientific data management and stewardship. Sci Data 3, 160018. https://doi.org/10.1038/sdata.2016.18

Williams, N.J., Jaramillo, P., Campbell, K., Musanga, B., Lyons-Galante, I., 2018. Electricity Consumption and Load Profile Segmentation Analysis for Rural Micro Grid Customers in Tanzania, in: 2018 IEEE PES/IAS PowerAfrica. Presented at the 2018 IEEE PES/IAS PowerAfrica, IEEE, Cape Town, pp. 360–365. https://doi.org/10.1109/PowerAfrica.2018.8521099

World Bank, 2021. Access to electricity (% of population) | Data [WWW Document]. URL https://data.worldbank.org/indicator/EG.ELC.ACCS.ZS (accessed 3.8.21).

World Bank, 2020. Population, total | Data [WWW Document]. URL https://data.worldbank.org/indicator/SP.POP.TOTL (accessed 10.14.21).

Yamegueu, D., Azoumah, Y., Py, X., Zongo, N., 2011. Experimental study of electricity generation by Solar PV/diesel hybrid systems without battery storage for off-grid areas. Renewable Energy 36, 1780–1787. https://doi.org/10.1016/j.renene.2010.11.011

Zeyringer, M., Pachauri, S., Schmid, E., Schmidt, J., Worrell, E., Morawetz, U.B., 2015. Analyzing grid extension and stand-alone photovoltaic systems for the cost-effective electrification of Kenya. Energy for Sustainable Development 25, 75–86. https://doi.org/10.1016/j.esd.2015.01.003

Figures

Figure 1

Modelling workflow

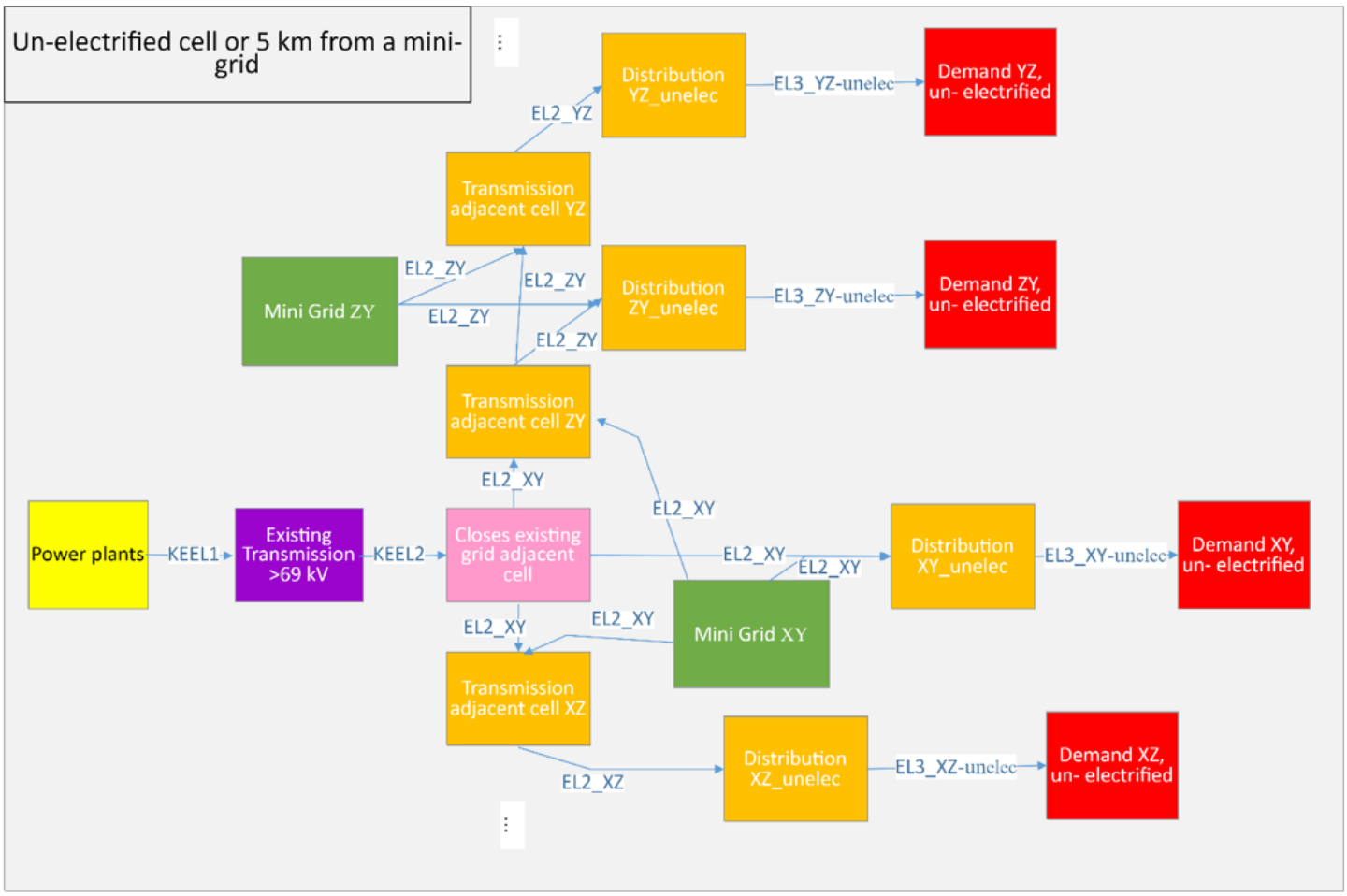

Figure 2

Expansion of transmission lines

Figure 3

Electrified settlements from electrification algorithm, 1x1 km cells

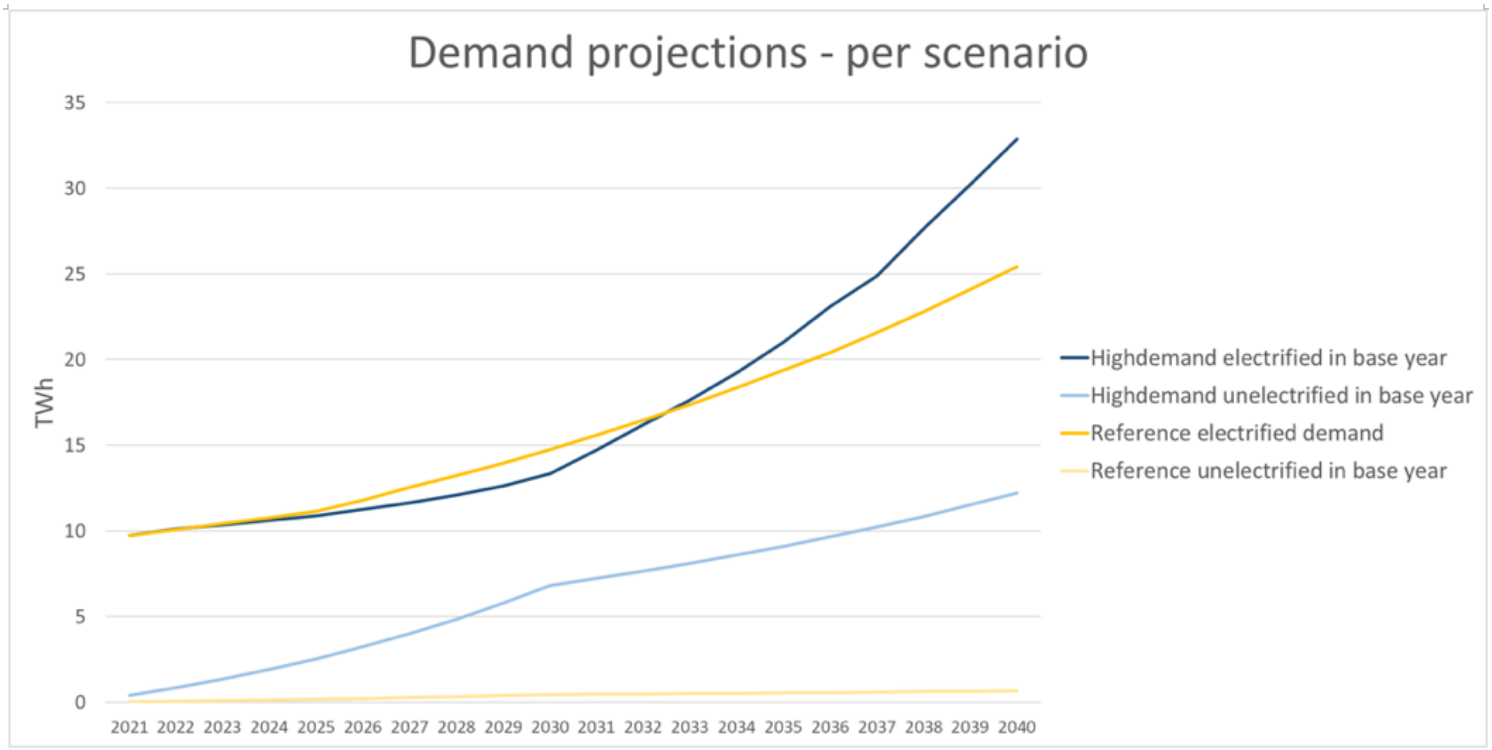

Figure 4

Modelled demand reference and high demand scenario

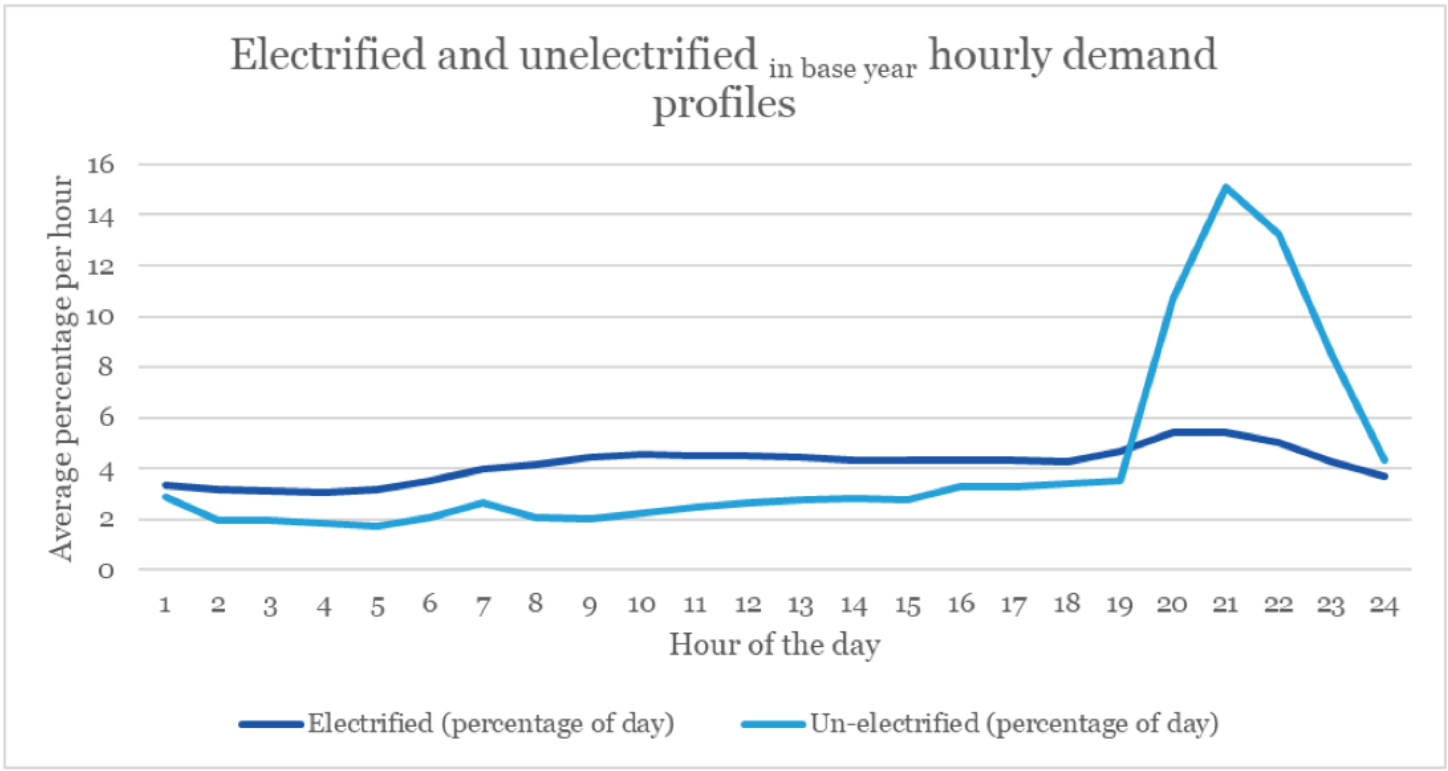

Figure 5

Electrified and un-electrified demand profile (unelectrified adapted from (Williams et al., 2018)) electrified from KLPC (KPLC, 2015)

Figure 6

Potential new distribution lines for un-electrified cells

Figure 7

Electricity flow between transmission lines in reference scenario over the years 2025, 2030 and 2035 in relation to the distribution lines expansion (GJ)

Figure 8

Electricity flow between transmission lines in high demand scenario over the years 2025, 2030 and 2035 in relation to the distribution lines expansion (GJ)

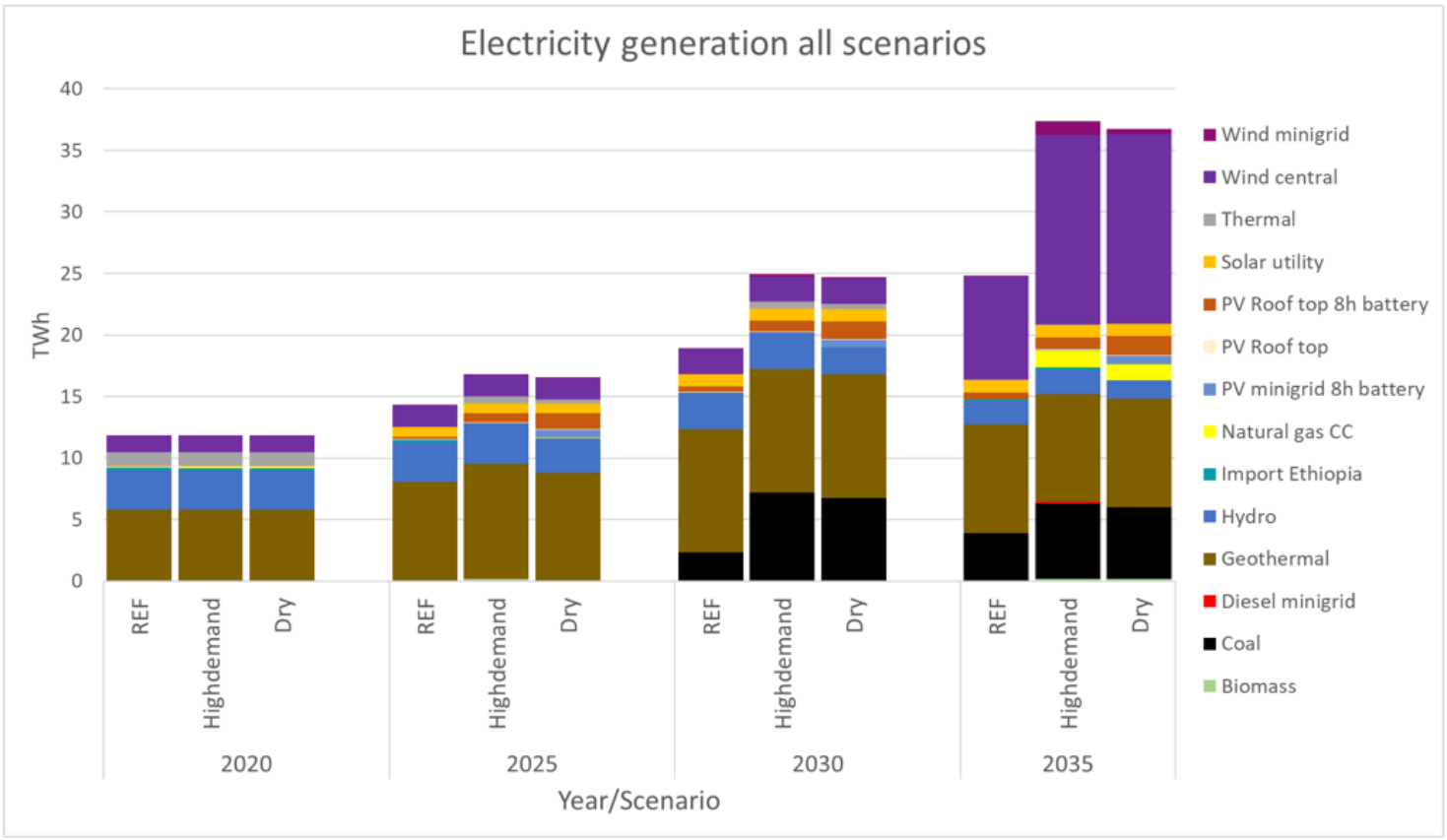

Figure 9

Electricity production for all three scenarios (TWh)

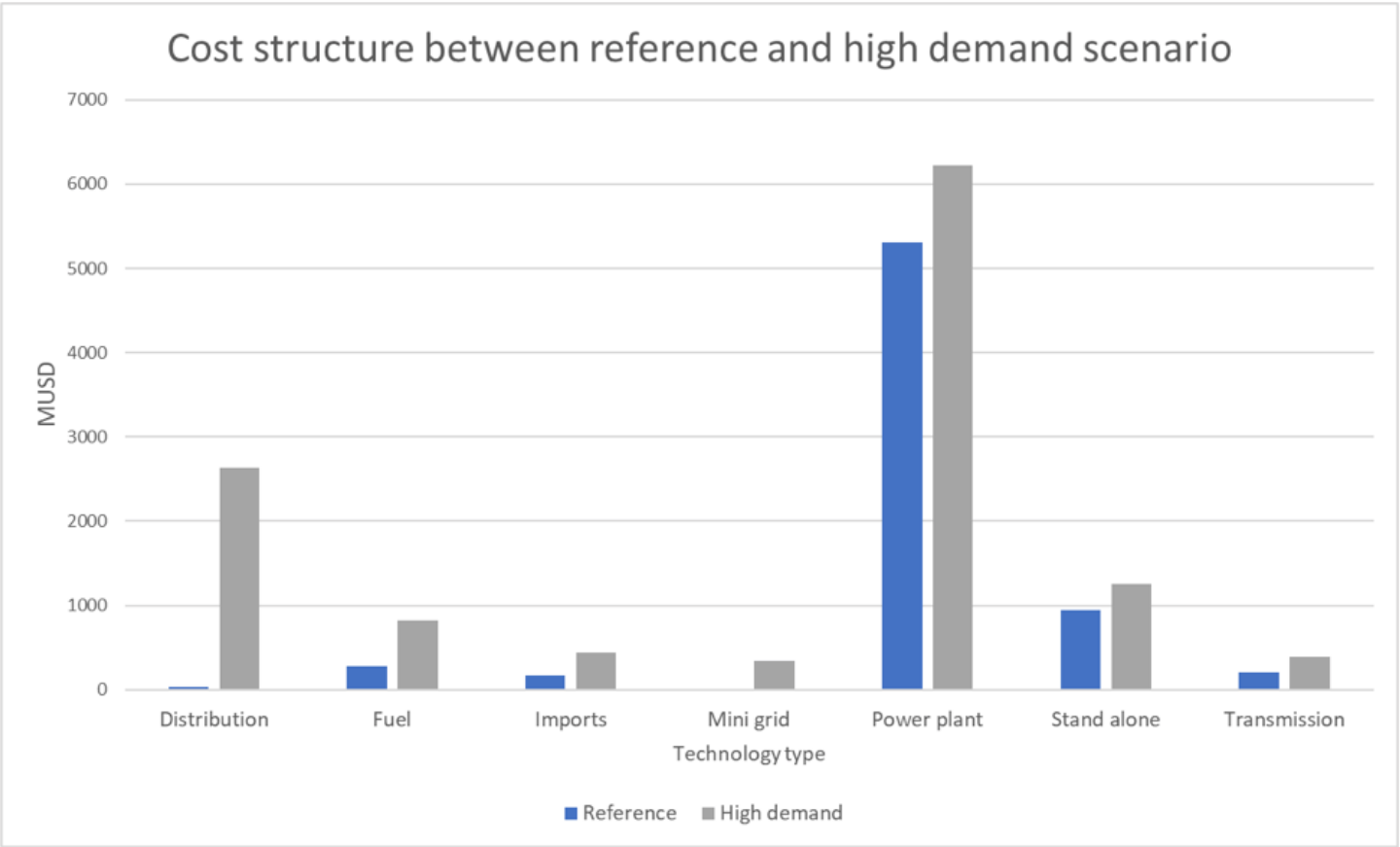

Figure 10

Total discounted cost for reference scenario and high demand scenario 2020-2040

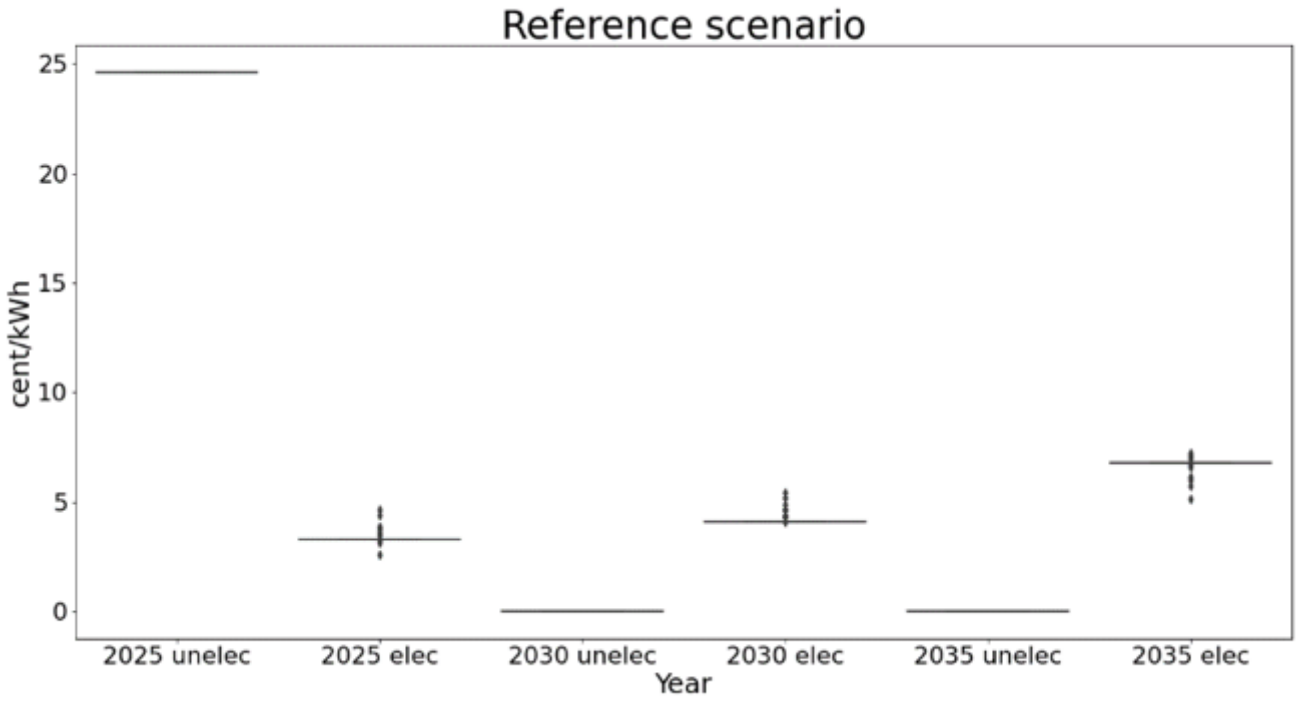

Figure 11

Shadow price for reference scenario 2025, 2030 and 2035

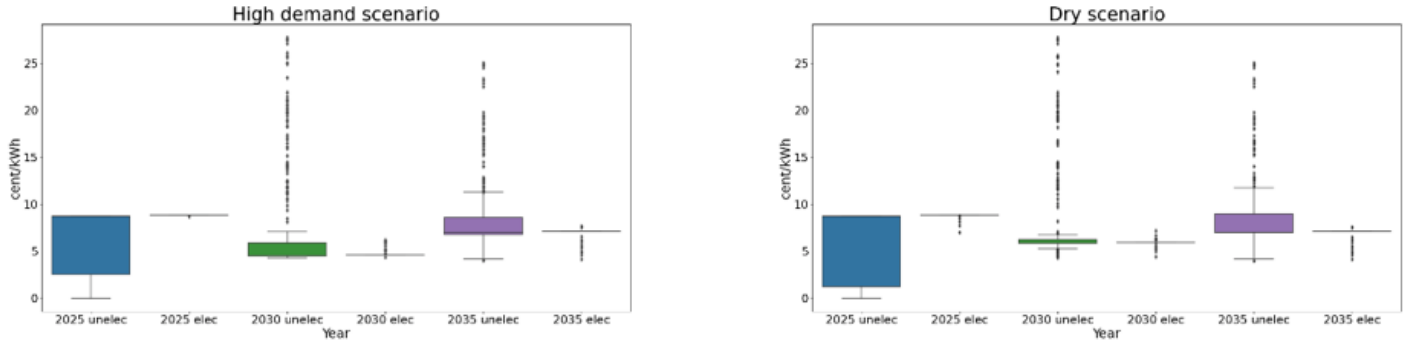

Figure 12

Shadow price for high demand and dry scenario in 2025, 2030, 2035

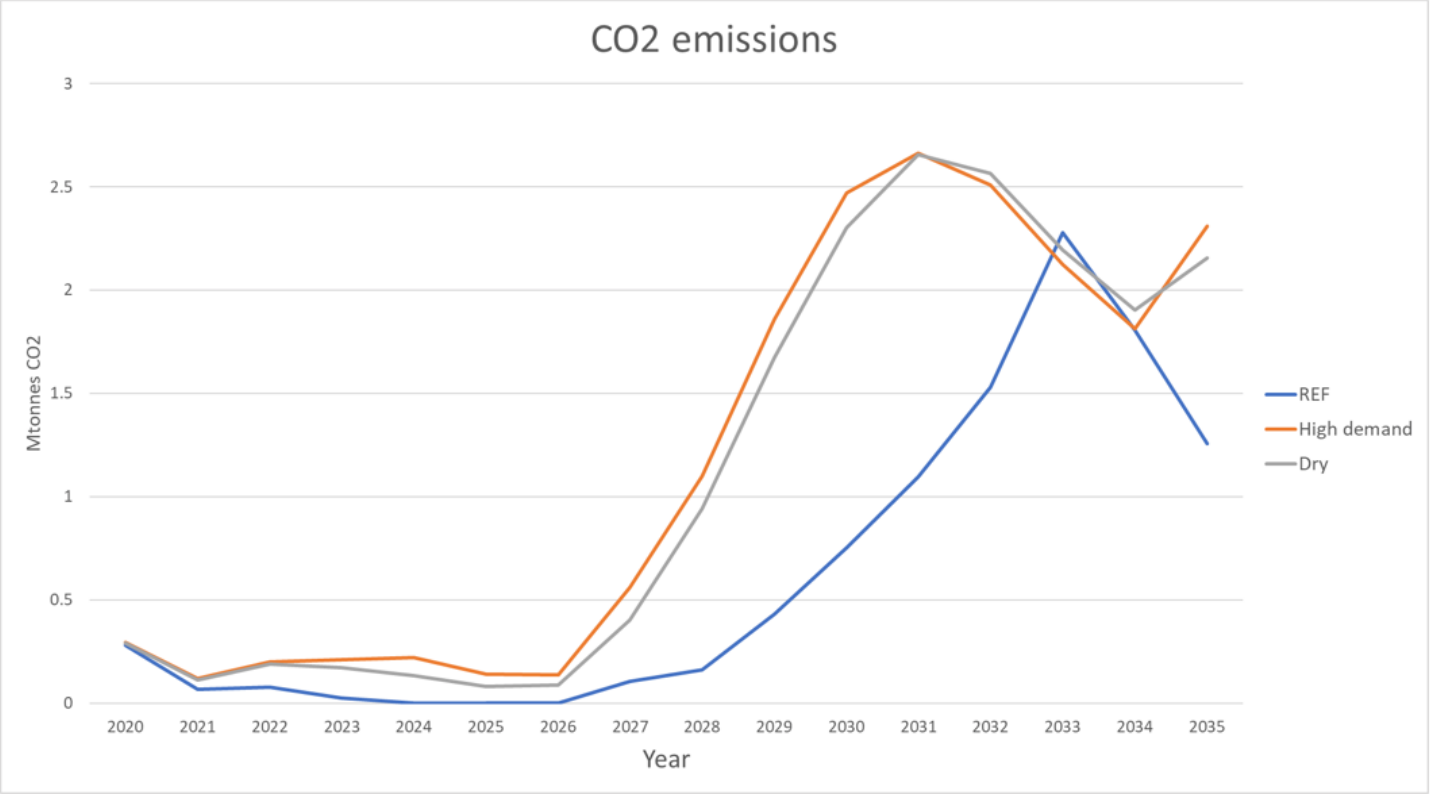

Figure 13

CO2 emissions per scenario

Supplementary Files

This is a list of supplementary files associated with this preprint. Click to download.

- Appendix.docx